Role of Atg1 in morphologic changes of the pathogenic fungus *Trichosporon asahii*

Mei Nakayama[1], Yasuhiko Matsumoto[1]*, Sanae Kurakado[1], Takashi Sugita[1]

[1]Department of Microbiology, Meiji Pharmaceutical University, 2-522-1, Noshio, Kiyose, Tokyo 204-8588, Japan.

*Corresponding author

E-mail: ymatsumoto@my-pharm.ac.jp (YM)

Short title: Atg1 and morphology of *T. asahii*

Abstract

Trichosporon asahii is a dimorphic fungus that causes severe invasive fungal infections, particularly in patients with neutropenia. Depending on nutrient availability, *T. asahii* exists in yeast, hyphae, or arthroconidia forms. Autophagy, a cellular degradation pathway responsible for removing old or damaged organelles, is essential for the survival of *Saccharomyces cerevisiae* under nutrient-limited conditions. Atg1 is a key regulator of the early phases of autophagy, especially under nitrogen starvation. The role of Atg1 in regulating morphology, stress resistance, or virulence in *T. asahii*, however, remains poorly understood. Here, we generated three *atg1* gene-deficient *T. asahii* mutants and investigated their phenotypic characteristics to reveal the role of Atg1 in *T. asahii*. The *atg1* gene-deficient mutants exhibited no growth defects under high-temperature or various chemical stress conditions, including antifungal drugs. Under a nutrient-rich culture condition, the mutants exhibited an increased proportion of hyphal cells. On the other hand, no morphologic differences were observed between the parent strain and the *atg1* gene-deficient mutants under a nitrogen-limited condition. The virulence of these *atg1* gene-deficient mutants was maintained in a silkworm infection model. Furthermore, all three generated *atg1* gene-deficient mutants exhibited consistent phenotypes. Our findings suggest that while Atg1 does not play a major role in stress tolerance or virulence in *T. asahii*, it plays a role in regulating its dimorphic morphologic changes.

Keywords: *Trichosporon asahii*, Atg1, morphology, virulence

34 # Introduction

35 *Trichosporon asahii* is a dimorphic fungus that exists in yeast, hyphal, and arthroconidia forms
36 [1]. *T. asahii* causes severe invasive fungal infections, particularly in immunocompromised hosts,
37 such as those with neutropenia [2–4]. While the mortality rate of invasive fungal infections caused
38 by the pathogenic fungus *Candida albicans* is approximately 40%, that caused by *T. asahii* is as
39 high as 70%–80% [5]. Furthermore, *T. asahii* exhibits tolerance to echinocandin antifungal agents
40 commonly used in clinical settings, often leading to breakthrough infections in patients receiving
41 micafungin [6]. The ability of *T. asahii* to form biofilms on medical device surfaces, such as
42 catheters, further complicates treatment by conferring resistance to various antifungal drugs and
43 contributing to chronic, treatment-resistant infections [7]. These characteristics of *T.*
44 *asahii* emphasize its clinical significance as a pathogenic fungus.

45 Autophagy is a conserved cellular process that maintains cellular homeostasis by
46 degrading and recycling cytoplasmic components, including damaged organelles and misfolded
47 proteins [8,9]. Autophagy is regulated by signaling pathways such as mTOR and AMPK and is
48 activated under stress conditions such as nutrient deprivation [10,11]. In the model
49 eukaryote *Saccharomyces cerevisiae*, autophagy plays a critical role in survival under nutrient-
50 limited conditions [12,13]. The process is initiated in response to nutrient deprivation, with Atg1
51 acting as a key regulator in its early stages [8,14]. Atg1 and other autophagy-related proteins are
52 essential for the progression of autophagy and are required for stress resistance and pathogenicity
53 in *Cryptococcus neoformans*, a basidiomycete closely related to *T. asahii* [15,16]. In *Candida*
54 *albicans*, another dimorphic fungus, Atg1 is required for biofilm formation [17,18]. The role of
55 the autophagy-related protein Atg1 in morphologic transitions, stress resistance, and virulence in *T.*
56 *asahii*, however, remains unclear.

57 In the present study, we independently generated three *atg1* gene-deficient mutants of *T.*
58 *asahii* and evaluated their morphology, stress sensitivity, and virulence. Our results revealed that
59 *atg1* gene deficiency promotes hyphal formation under nutrient-rich conditions but does not affect
60 growth under various stress conditions or virulence in the silkworm infection model. These
61 findings suggest that Atg1 is involved in regulating the morphologic changes of *T. asahii*.
62

63 Materials & Methods

64 *T. asahii* strains

65 *T. asahii* MPU129Δ*ku70* was used as the parental strain [19]. Three independent *T. asahii*
66 *atg1* gene-deficient mutants were generated in this study (Table 1).
67

68 Culture conditions for *T. asahii*

69 *T. asahii* strains were cultured according to previously described methods [19]. *T. asahii* strains
70 were grown on Sabouraud dextrose agar (SDA; 1% hipolypeptone, 4% dextrose, and 1.5% agar)
71 containing G418 (100 μg/mL) and cefotaxime (100 μg/mL) at 27°C for 1–2 days.
72

73 Reagents

74 Nourseothricin was purchased from JENA BIOSCIENCE GMBH (Dortmund, Germany).
75 Fluconazole was purchased from Tokyo Chemical Industry Co., Ltd. (Tokyo, Japan). Cefotaxime
76 sodium, D-glucose, agar, NaCl, sorbitol, H_2O_2, dithiothreitol (DTT), and Yeast Nitrogen Base
77 without Amino Acids and Ammonium Sulfate were obtained from FUJIFILM Wako Pure
78 Chemical Corporation (Osaka, Japan). Congo red was purchased from Sigma-Aldrich Co., LLC

79 (St. Louis, MO, USA). G418 was obtained from Enzo Life Science, Inc. (Farmingdale, NY, USA).
80 Hipolypeptone was purchased from NIHON PHARMACEUTICAL Co., LTD. (Tokyo, Japan).
81 Tunicamycin was purchased from Cayman Chemical Company (Ann Arbor, MI, USA).
82 Amphotericin B and KCl were obtained from Wako Pure Chemical Industries, Ltd. (Osaka, Japan).
83 Sodium dodecyl sulfate (SDS) was purchased from NIPPON GENE Co., LTD. (Tokyo, Japan).
84 Tween 80 was obtained from MP Biomedicals LLC (Santa Ana, CA, USA).
85

86 Conservation of Atg1 protein amino acid sequence in *T. asahii* and other fungi

87 Homology and domain analyses were performed as previously described [20]. The amino acid
88 sequence of the *T. asahii* Atg1 protein was obtained from the National Center for Biotechnology
89 Information (NCBI) (https://www.ncbi.nlm.nih.gov/). BLASTp
90 (https://blast.ncbi.nlm.nih.gov/Blast.cgi) was used to compare the sequence homology with the
91 Atg1 proteins of *C. albicans*, *A. fumigatus*, *C. neoformans*, and *S. cerevisiae*. A phylogenetic tree
92 was constructed using the maximum likelihood method with MEGA11 Software
93 (https://www.megasoftware.net/). The NCBI gene accession numbers of Atg1 proteins used for
94 phylogenetic analysis and alignment are listed in Table 2. The NCBI domain accession numbers
95 used for functional domain analysis and alignment are shown in Table 3.
96

97 Generation of *atg1* gene-deficient *T. asahii* mutants

98 Generation of the gene-deficient *T. asahii* mutants was performed according to previously
99 described methods [21]. The pUC19-*atg1* (5'UTR) -*NAT1*-*atg1* (3'UTR) plasmid was constructed
100 using the In-Fusion method. Approximately 1200 bp of the 5′-UTR and 3′-UTR regions of
101 the *atg1* gene were cloned upstream and downstream of the *NAT1* gene region in the pUC19-

102 NAT1 vector using the In-Fusion method (In-Fusion Snap Assembly Master Mix; Takara Bio Inc.,
103 Shiga, Japan). Using the pUC19-*atg1* (5'UTR) -*NAT1*-*atg1* (3'UTR) plasmid, polymerase chain
104 reaction (PCR) was performed to amplify a DNA fragment containing *atg1* (5'UTR) -*NAT1*-*atg1*
105 (3'UTR). The primers used for PCR are listed in Table 4. Gene transfer to *T. asahii* cells was
106 performed as described previously with modifications [22]. The parental strain was cultured on
107 SDA at 27°C for 1 day. Cells on the agar medium were suspended in 2 mL of saline and filtered
108 through a 40-µm cell strainer. The filtered suspension was centrifuged at 10,000 rpm for 5 min,
109 and the pellet was resuspended in 1 mL of distilled water and centrifuged again under the same
110 conditions. This washing step was repeated four times. The washed cells were then suspended in
111 1 mL of 1.2 M sorbitol solution and centrifuged at 10,000 rpm for 5 min. The harvested pellet was
112 resuspended in 40 µL of 1.2 M sorbitol to obtain competent cells. To perform electroporation, 4
113 µL of the PCR-amplified *atg1* (5'UTR) -*NAT1*-*atg1* (3'UTR) DNA fragment was added to 40 µL
114 of the competent cells and incubated on ice for 15 min. The mixture was transferred to a 2-mm
115 gap cuvette (Bio-Rad Laboratories, Inc., CA, USA), and electroporation was performed using a
116 Gene Pulser Xcell (Bio-Rad Laboratories, Inc., CA, USA) with the time constant protocol (1800
117 V, 5 ms). After electroporation, 500 µL of Yeast Polypeptone Dextrose (YPD) medium (2%
118 hipolypeptone, 1% yeast extract, 2% glucose) containing 0.6 M sorbitol was added, and the cells
119 were incubated at 27°C for 3 h. After incubation, the cells were plated on SA medium containing
120 nourseothricin (300 µg/mL) and incubated at 27°C for 3 days. Genomic DNA was extracted from
121 the nourseothricin-resistant transformants, and deletion of the *atg1* gene was confirmed by PCR.
122

123 **Temperature sensitivity test**

124 A temperature sensitivity test was performed as described previously with modifications [22]. *T.*

125 *asahii* strains were grown on SDA containing cefotaxime (100 μg/mL) at 27°C for 1 day. *T. asahii*
126 cells were suspended in saline, and the absorbance at 630 nm was adjusted to 1. A 10-fold serial
127 dilution of each suspension was prepared using saline. Five microliters of each dilution were
128 spotted onto SDA and incubated at 27°C, 37°C, or 40°C for 48 h. Photographs of the agar plates
129 were taken after incubation. For evaluation in liquid culture, Sabouraud dextrose broth (1%
130 hipolypeptone, 4% dextrose) was used. *T. asahii* cells were suspended in saline and filtered
131 through a 40-μm cell strainer. Absorbance at 630 nm was adjusted to 0.005. The suspensions were
132 incubated at 27°C, 37°C, or 40°C for 96 h, and absorbance at 630 nm was measured every 24 h
133 using a microplate reader (iMark™ microplate reader; Bio-Rad Laboratories Inc., Hercules, CA,
134 USA).
135

136 **Drug sensitivity test**

137 A drug sensitivity test was performed as previously reported with modifications [20]. *T. asahii* was
138 grown on SDA containing cefotaxime (100 μg/mL) at 27°C for 2 days. Cells were suspended in
139 saline and filtered through a 40-μm cell strainer. Absorbance of the suspension was adjusted to 1.0
140 at 630 nm. A 10-fold serial dilution of each suspension was prepared using saline. Five microliters
141 of each dilution were spotted onto SDA containing NaCl, KCl, Congo red, SDS, H_2O_2,
142 tunicamycin, DTT, amphotericin B, or fluconazole. The plates were incubated at 27°C or 37°C for
143 24 to 72 h, and images of the agar plates were captured after incubation.

144 The minimum inhibitory concentration (MIC) was determined using the broth
145 microdilution method according to CLSI guideline M27-A3, with a commercial antifungal
146 susceptibility testing plate for yeasts (DP Eiken; Eiken Chemical Co., Ltd., Tokyo, Japan) [20]. *T.*
147 *asahii* was grown on SDA containing cefotaxime (100 μg/mL) at 27°C for 2 days. The cells were

148 suspended in saline and adjusted to a turbidity equivalent to McFarland standard 1. The
149 suspensions were then diluted 20-fold with saline, followed by a 100-fold dilution with RPMI
150 1640 medium (Thermo Fisher Scientific Inc., MA, USA) supplemented with 0.165 M 3-
151 morpholinopropane-1-sulfonic acid (RPMI-MOPS, pH 7.0; FUJIFILM Wako Pure Chemical
152 Corporation, Osaka, Japan). A 100-μL volume of the prepared cell suspension was added to each
153 well of the plate containing one of the following eight antifungal agents: micafungin, caspofungin,
154 amphotericin B, 5-fluorocytosine, fluconazole, itraconazole, voriconazole, or miconazole. The
155 plates were incubated at 37°C for 48 h. MIC values were determined based on the results of two
156 independent experiments.
157

158 **Morphologic analysis of *T. asahii***

159 *T. asahii* strains were grown on SDA containing cefotaxime (100 μg/mL) at 27°C for 2 days. *T.*
160 *asahii* cells were suspended in saline and filtered through a 40-μm cell strainer. Absorbance of the
161 suspension was adjusted to 1.0 at 630 nm. A 20-μL aliquot of the suspension was added to 200 μL
162 each of the Sabouraud dextrose broth (SB) and Synthetic Defined – Nitrogen (SD–N) medium.
163 The cells were incubated at 37°C for 24 h. After incubation, culture samples were placed on
164 microscope slides, covered with coverslips, and observed under a light microscope (BX51;
165 OLYMPUS Corp., Tokyo, Japan). Photographs of the cells were randomly captured from multiple
166 microscopic fields. The *T. asahii* morphology was classified as follows: yeast form, observed as
167 single, spherical cells including budding yeasts; arthroconidia, observed as chains of three or more
168 round or rectangular cells separated by septa; hyphal form, observed as elongated structures at
169 least twice the length of yeast cells, including pseudohyphae, but lacking septa characteristic of

170 arthroconidia [20,23]. More than 400 cells were observed, and the number of each morphologic
171 type (yeast, arthroconidia, hyphae) was counted.
172

173 ## Silkworm infection experiments

174 Silkworm infection experiments were performed according to previously described methods with
175 modifications [22]. Silkworm eggs (KINSYU X SHOWA) were purchased from Ehime-Sanshu
176 Co., Ltd. (Ehime, Japan), disinfected, and incubated at 25–27°C until hatching. The hatched larvae
177 were reared on an artificial diet, SilkMate 2S (Nosan Corp., Kanagawa, Japan). Fifth-instar
178 silkworm larvae were fed SilkMate 2S overnight before use in the infection experiments. *T.*
179 *asahii* was grown for 1 day at 27°C on SDA containing cefotaxime (100 μg/mL). Cells were
180 suspended in saline and filtered through a 40-μm cell strainer. Absorbance of the resulting
181 suspension at 630 nm was adjusted to 1. The cell suspension was then diluted 250-fold with saline,
182 and 50 μL of the diluted suspension was injected into the silkworm hemolymph from the dorsal
183 side using a 1-mL tuberculin syringe (Terumo Medical Corporation, Tokyo, Japan). The silkworms
184 were fed SilkMate 2S and maintained in a 37°C incubator, where their survival was monitored.
185

186 ## Statistical analysis

187 All experiments were performed at least twice, and representative results are shown. For
188 morphologic analysis, differences between groups were analyzed by Dunnett's test. For silkworm
189 infection assays, differences between groups were analyzed using the log-rank test based on
190 Kaplan–Meier survival curves generated with EZR version 1.5.5 (https://www.jichi.ac.jp/saitama-
191 sct/SaitamaHP.files/download.html). A P-value of < 0.05 was considered statistically significant.
192

193 # Results

194 ## Identification and conservation of the Atg1 Protein in *T. asahii*

195 We sought to identify a gene encoding a homologous Atg1 protein in the *T. asahii* genome. In *C.*
196 *neoformans*, *atg1* was identified based on the amino acid sequence of the *S. cerevisiae* Atg1 protein
197 [11,16]. *T. asahii* hypothetical protein A1Q1_02656 was identified as a candidate protein with
198 52% amino acid identity to *C. neoformans* Atg1 (Table 2). Next, we performed a homology
199 analysis comparing the amino acid sequence of *T. asahii* hypothetical protein A1Q1_02656 with
200 Atg1 proteins from representative fungi such as *S. cerevisiae*, *A. fumigatus,* and *C. albicans*. *T.*
201 *asahii* hypothetical protein A1Q1_02656 showed 52%, 52%, 50%, and 47% amino acid identity
202 with Atg1 proteins of *C. neoformans*, *A. fumigatus*, *C. albicans*, and *S. cerevisiae*, respectively
203 (Figure 1A, Table 2). A phylogenetic tree generated from these amino acid sequences revealed
204 that, among the fungi analyzed, *T. asahii* hypothetical protein A1Q1_02656 was most closely
205 related to *C. neoformans* Atg1 (Fig. 1B). Functional domain analysis revealed that the *T.*
206 *asahii* hypothetical protein A1Q1_02656 also contained a PKc_like superfamily domain, a
207 catalytic domain of protein kinases (Fig. 1C, Table 3). Therefore, the *T. asahii* hypothetical protein
208 A1Q1_02656 was estimated to be the Atg1 protein in *T. asahii,* and the corresponding gene was
209 designated *atg1*.

210

211 **Fig. 1. Conservation of *T. asahii* Atg1 among fungi.**

212 (**A**) Phylogenetic tree of Atg1 proteins from *T. asahii*, *C. neoformans*, *A. fumigatus*, *C. albicans*,
213 and *S. cerevisiae*, constructed using the maximum likelihood method. (**B**) Phylogenetic tree of
214 Atg1 proteins from *T. asahii*, *C. neoformans*, *A. fumigatus*, *C. albicans*, and *S. cerevisiae*,
215 constructed using the maximum likelihood method. Phylogenetic analysis was performed using

216 MEGA11 Software (https://www.ncbi.nlm.nih.gov/). (**C**) Schematic diagrams of domains present
217 in Atg1 proteins. PKc: PKc_like superfamily domain. STKc: STKc_ATG1_ULK_like domain.
218 HB: Herpes_BLLF1 superfamily domain. DUF: DUF3543. Functional domain prediction was
219 performed using the National Center for Biotechnology Information (NCBI)
220 (https://www.ncbi.nlm.nih.gov/).
221

222 Generation of *atg1* gene-deficient *T. asahii* mutants

223 The gene-targeting method used to generate gene-deficient *T. asahii* mutants was established
224 previously [19][24]. Using the method, we generated three *atg1* gene-deficient *T. asahii* mutants.
225 The DNA fragment used for *atg1* gene deletion contained the *NAT1* gene, which confers resistance
226 to nourseothricin (Fig. 2A). Homologous recombination replaced the *atg1* gene with
227 the *NAT1* gene, thereby conferring resistance to nourseothricin (Fig. 2B). Transformation was
228 performed by introducing the DNA fragment into the parental strain via electroporation, and
229 transformants resistant to nourseothricin were obtained (Fig. 2B). Genomic DNA was extracted
230 from the nourseothricin-resistant transformants, and *atg1* gene deficiency was confirmed by PCR
231 (Fig. 2C, D). These results suggest that the *atg1* gene-deficient *T. asahii* mutants were generated.
232

233 **Fig. 2. Generation of the *atg1* gene-deficient *T. asahii* mutants.**
234 (**A**) Schematic diagram of the gene recombination strategy used to construct the *atg1* gene-
235 deficient *T. asahii* mutant (Δ*atg1*), along with the predicted genomic structure of the *atg1* gene-
236 deficient mutant. (**B**) The parental strain (Parent) and the *atg1* gene-deficient mutants (Δ*atg1* #1-
237 3) were spread on SDA or SDA containing nourseothricin (100 µg/mL; Nou (+)) and incubated at
238 27°C for 2 days. (**C**) Schematic illustration of primer positions and expected amplified DNA

239 fragment sizes by PCR to verify the genomic structure of the *atg1* gene-deficient candidates using
240 extracted genomic DNA. (**D**) DNA electrophoresis of PCR products to confirm the *atg1* gene
241 deficiency (Δ*atg1*).
242

243 Effects of *atg1* gene deficiency on stress sensitivity

244 Next, we investigated whether growth of the *atg1* gene-deficient mutants was similar to that of the
245 parental strain. Under temperatures of 27°C, 37°C, or 40°C, no significant differences in growth
246 were observed between the parental strain and the *atg1* gene-deficient mutants (Fig. 3). In *C.*
247 *neoformans*, mutants lacking autophagy-related genes exhibit sensitivity to oxidative and osmotic
248 stress [15]. To evaluate whether the *T. asahii atg1* gene is involved in osmotic stress, cell
249 wall/membrane stress, endoplasmic reticulum stress, or oxidative stress, stress sensitivity assays
250 were performed. The growth of the *atg1* gene-deficient mutants was not altered under the tested
251 compounds (Fig. 4). The MICs of antifungal agents for the *atg1* gene-deficient strains were
252 comparable to those for the parental strain (Table 5). These results suggest that the *atg1* gene is
253 not involved in susceptibility to compound-induced stresses and antifungal agents in *T. asahii*.
254

255 **Fig. 3. Growth of the *atg1* gene-deficient *T. asahii* mutants under high-temperature**
256 **conditions.**
257 (**A**) The parental strain (Parent) and the *atg1* gene-deficient *T. asahii* mutants (Δ*atg1* #1-3) were
258 grown on SDA at 27°C for 2 days. Cells were suspended in saline, and 10-fold serial dilutions
259 were prepared. Each dilution (5 μl) was spotted onto SDA and incubated at 27°C, 37°C, or 40°C
260 for 48 h. (**B**) The parental strain (Parent) and the *atg1* gene-deficient *T. asahii* mutants (Δ*atg1* #1-

261 3) were grown in Sabouraud dextrose broth at 27°C, 37°C, or 40°C, and absorbance at 630 nm
262 was measured. Data are presented as mean ± standard error of the mean (SEM).
263
264 **Fig. 4. Growth of the *atg1* gene-deficient *T. asahii* mutants under stress-inducing conditions.**
265 The parental strain (Parent) and the *atg1* gene-deficient *T. asahii* mutants (Δ*atg1* #1-3) were
266 cultured on SB at 27°C for 2 days. Cells were suspended in saline, and 10-fold serial dilutions
267 were prepared. Each dilution (5 μL) was spotted onto SA medium containing NaCl (1 M), KCl
268 (1.5 M), Congo red (300 μg/mL), SDS (0.01%), tunicamycin (TM, 1 μg/mL), dithiothreitol (DTT,
269 15 mM), or hydrogen peroxide (H_2O_2, 4 mM), and incubated at 27°C for 48 h.
270

271 Role of the *atg1* gene in *T. asahii* morphology

272 *T. asahii* exhibits dimorphism, alternating between yeast forms and filamentous/arthroconidial
273 forms [1]. In *C. albicans*, a dimorphic fungus, hyphal formation is induced by various nutritional
274 conditions, such as growth at 37°C and exposure to GlcNAc [25]. To observe the morphologic
275 changes of *T. asahii* yeast cells under various nutritional conditions, we developed a method to
276 collect *T. asahii* yeast cells. More than 90% of *T. asahii* cells in suspension filtered through a 40-
277 μm filter were yeast cells (Fig. 5A, B). Using the *T. asahii* yeast cells, we tested the growth of the
278 cells in various culture media, such as SB and SD-N. The absorbance of *T. asahii* culture medium
279 at 630 nm was increased in the order SB and SD-N (Fig. 5C). The ratio of hyphae was increased
280 in SB by incubating at 37°C for 24 h (Fig. 5D, E). The ratio of arthroconidia was also increased
281 by incubation in SB and SD-N at 37°C for 24 h (Fig. 5D, E). We investigated whether the *atg1*
282 gene contributes to the morphologic changes of *T. asahii* in various culture media. The *atg1* gene-
283 deficient mutants exhibited a higher proportion of hyphal cells in SB (Fig. 6). No significant

284 morphologic differences were observed, however, between the parental strain and the *atg1*-
285 deficient *T. asahii* mutants in SD-N (Fig. 6). These results suggest that the *atg1* gene negatively
286 regulates hyphal formation in *T. asahii* in a nutrient-dependent manner.
287
288 **Fig. 5 Effects of culture conditions on *T. asahii* morphology.**
289 (**A**) Method for preparing the yeast form of *T. asahii*. The parental *T. asahii* strain (Parent) was
290 cultured on SDA at 27°C for 2 days. *T. asahii* cells were suspended in saline and filtered through
291 a 40-μm cell strainer. (**B**) The ratio of each cell shape in the filtered *T. asahii* cells was measured.
292 (**C**) Absorbance of the cell suspension at 630 nm was adjusted to 0.5, and 5 μL of the filtered cell
293 suspension was added to 200 μL of Sabouraud dextrose medium or SD-N liquid medium. Cultures
294 were incubated at 27°C for 24 h, and absorbance at 630 nm was measured for 24 h. (**D-F**)
295 Absorbance of the filtered cell suspension at 630 nm was adjusted to 1.0, and 20 μL of the
296 suspension was added to 200 μL of Sabouraud dextrose broth (SB) or synthetic defined-nitrogen
297 (SD–N) medium, followed by incubation at 27°C for 24 h. Cells were then observed under a light
298 microscope. Scale bars represent 40 μm. Images were captured randomly from multiple
299 microscopic fields. Cell numbers in three morphologic categories: yeast, arthroconidia, and hyphae,
300 were quantified. (**D**) Cell numbers in three morphologic categories were measured at 0 or 24 h
301 after incubation at 37°C. (**E**) Photographs of cells after incubation at 37°C for 24 h were obtained
302 under microscopic fields. *n* represents the total number of microscopic fields analyzed from two
303 independent experiments.
304
305 **Fig. 6. Effect of *atg1* gene deficiency on *T. asahii* morphology.**
306 The parental *T. asahii* strain (Parent) and three *atg1* gene-deficient mutants (Δ*atg1* #1-3) were

307 grown on SDA at 27°C for 2 days. Cells were suspended in saline and filtered through a 40-μm
308 cell strainer. Absorbance at 630 nm was adjusted to 1. A 20-μL aliquot of each suspension was
309 added to (**A**) Sabouraud dextrose broth (SB), or (**B**) synthetic defined-nitrogen (SD–N) medium
310 (200 μL). The samples were incubated at 37°C for 24 h. After incubation, the *T. asahii* cells were
311 dropped onto microscope slides, covered with coverslips, and observed under a light microscope.
312 Upper panels show representative microscopic images. Scale bars represent 20 μm. Lower panels
313 show quantification of the three morphologic forms—yeast, arthroconidia, and hyphae—based on
314 randomly selected microscopic fields. The total number of cells was obtained from two
315 independent experiments. (**C**) The relative ratio of the three morphologic forms were determined
316 compared to the ratio of parental strain (Parent) under a culture condition with SB at 37°C for 24
317 h. The data of the relative ratio were obtained from seven independent experiments. Error bars
318 indicate the SEM of the means (n = 7). Statistical differences between parental strain and Δ*atg1*
319 #1-3 were analyzed by Dunnett's test. (*: $P < 0.05$).
320

321 **Virulence of the *atg1* gene-deficient mutants in a silkworm infection model**

322 In *C. neoformans*, *atg1 g*ene deficiency did not affect its virulence in a *Galleria mellonella*
323 infection model [15]. We tested whether the *atg1* gene is required for *T. asahii* virulence in a
324 silkworm infection model. The survival time of silkworms infected with the *atg1*-deficient mutants
325 was not significantly different from that of silkworms infected with the parental strain (Fig. 7).
326 The result suggests that the *atg1* gene does not contribute to *T. asahii* virulence in the silkworm
327 model.
328

329 **Fig. 7. Virulence of *T. asahii atg1* gene-deficient mutants in a silkworm infection model.**
330 The parental strain (Parent; 530 cells/larva) and three independent *atg1* gene-deficient *T. asahii*
331 mutants (Δ*atg1* #1-3; 790 - 950 cells/larva) were injected into the hemocoel of silkworms, and
332 survival was monitored at 37°C for 96 h. Statistical significance between the parental and *atg1*-
333 deficient groups was determined by the log-rank test based on Kaplan–Meier survival curves. Ten
334 silkworms per group were used.
335

336 # Discussion

337 The findings of the present study demonstrated that the *atg1* gene is involved in morphologic
338 transitions of *T. asahii* under nutrient-rich conditions. On the other hand, *atg1* gene deficiency did
339 not affect growth under various stress conditions or virulence of *T. asahii* in the silkworm model.
340 These findings suggest that Atg1 might play a role in regulating hyphal formation under specific
341 culture conditions but is not involved in stress resistance or virulence in *T. asahii*.
342 *T. asahii* Atg1 protein was estimated based on the amino acid sequence of other fungal
343 Atg1 proteins and their domain analysis. *T. asahii* hypothetical protein A1Q1_02656 has high
344 sequence similarity to the Atg1 proteins of other representative fungi, including *S. cerevisiae*, *A.*
345 *fumigatus*, and *C. albicans*. Domain analysis revealed that *T. asahii* hypothetical protein
346 A1Q1_02656 harbors a Pkc_like superfamily domain—a catalytic domain of protein kinases
347 conserved among the analyzed fungi. In *S. cerevisiae*, Atg1 kinase activity contributes to non-
348 selective autophagy [8]. Therefore, we determined that *T. asahii* hypothetical protein A1Q1_02656
349 is the Atg1 protein of *T. asahii*.
350 *T. asahii atg1* gene deficiency does not significantly affect the stress response and
351 antifungal drug resistance of *T. asahii*. We generated *atg1* gene-deficient *T. asahii* mutants and

352 analyzed their phenotypes. When generating gene-deficient mutants, unintended secondary
353 mutations may be introduced in addition to the targeted gene disruption. To minimize the
354 possibility of this rare occurrence, we generated three independent *T. asahii atg1* gene-deficient
355 mutants in this study and examined whether they exhibited consistent phenotypes. The *atg1* gene
356 deficiency in *T. asahii* did not affect sensitivity to high temperature, NaCl, KCl, tunicamycin, DTT,
357 H_2O_2, or antifungal drugs. In *C. neoformans*, the *atg1* gene-deficient mutant also did not exhibit
358 high-temperature and H_2O_2-sensitive phenotypes [15,16]. Therefore, the *atg1* gene is not involved
359 in high temperature and oxidative stress tolerance in *T. asahii* or *C. neoformans*. On the other hand,
360 in *C. neoformans*, the growth of the *atg1* gene-deficient mutant was delayed by NaCl [15]. The
361 *atg1* genes in *T. asahii* and *C. neoforman*s might differ in their tolerance to NaCl. The calcineurin
362 and Hog1 pathways are involved in high-temperature tolerance in *T. asahii* [19,20]. We therefore
363 concluded that the *T. asahii* Atg1 is regulated in a calcineurin and Hog1 pathway-independent
364 manner.

365 The *atg1* gene contributes to the morphologic changes of *T. asahii*. In SB, the ratio of
366 hyphae was increased by *atg1* gene deficiency after 24-h incubation. On the other hand, in SD-N,
367 a nitrogen-limited medium, the morphology in the *atg1* gene-deficient mutants was not different
368 from that in the parental strain. In fungi such as *S. cerevisiae*, *C. neoformans*, and *C. albicans*,
369 Atg1 is involved in nitrogen limitation-induced autophagy and required for survival under
370 nitrogen-limited conditions [26]. In the present study, we revealed the role of Atg1 in the
371 morphologic changes of *T. asahii* under nutrient-rich conditions. Further studies are needed to
372 elucidate the intracellular mechanisms regulated by Atg1 under nutrient-rich conditions.

373 The *T. asahii atg1* gene is not involved in *T. asahii* virulence in the silkworm infection
374 model. In *C. neoformans*, Atg1 does not influence virulence in the insect model *Galleria*

375 *mellonella* [15]. Therefore, we assume that Atg1 does not have a pivotal role in *T. asahii* and *C.*
376 *neoformans* virulence in insect models.

377 A limitation of this study is that the effects of *atg1* gene-deficiency of *T. asahii* on
378 autophagy were not evaluated. Autophagy validation methods have been established in several
379 fungi using fungal cells expressing GFP-Atg8 [27]. The development of a detection system for
380 autophagy in *T. asahii* using cells expressing GFP-Atg8–expressing cells remains a future
381 challenge.

382

383 # Conclusion

384 The *atg1* gene contributes to the morphologic changes of *T. asahii* under nutrient-rich conditions.
385 Hyphal formation of *T. asahii* might be partially regulated by Atg1-dependent cellular events.

386

387 # Acknowledgements

388 We thank Renta Endo, Momoka Matsumura, and Tomoya Sanbongi (Meiji Pharmaceutical
389 University) for technical assistance rearing the silkworms. We also thank the editors of
390 SciTechEdit International LLC (Highlands Ranch, CO, USA) for English-language editing.

391

392 # Funding

393 This study was supported by JSPS KAKENHI grant number JP23K06141 (Scientific Research (C)
394 to Y.M.) and in part by the Research Program on Emerging and Re-emerging Infectious Diseases
395 of the Japan Agency for Medical Research and Development, AMED (Grant number
396 JP23fk0108679h0401 to T.S.).

397

398 # References

399 1. Colombo AL, Padovan ACB, Chaves GM. Current knowledge of trichosporon spp. and
400 trichosporonosis. Clinical Microbiology Reviews. 2011 Oct;24(4):682-700.
401 2. Walsh TJ, Lee JW, Melcher GP, Navarro E, Bacher J, Callender D, et al. Experimental
402 *Trichosporon* infection in persistently granulocytopenic rabbits: implications for
403 pathogenesis, diagnosis, and treatment of an emerging opportunistic mycosis. J Infect Dis.
404 1992 Jul;166(1):121-33.
405 3. Walsh TJ, Melcher GP, Lee JW, Pizzo PA. Infections due to Trichosporon species: new
406 concepts in mycology, pathogenesis, diagnosis and treatment. Curr Top Med Mycol.
407 1993;5:79-113.
408 4. Duarte-Oliveira C, Rodrigues F, Gonçalves SM, Goldman GH, arvalho A, Cunha C. The
409 cell biology of the Trichosporon-host interaction. Front Cell Infect Microbiol. 2017 Apr
410 7;7:118.
411 5. Krcmery V Jr, Mateicka F, Kunová A, Spánik S, Gyarfás J, Sycová Z, et al. Hematogenous
412 trichosporonosis in cancer patients: report of 12 cases including 5 during prophylaxis with
413 itraconazol. Support Care Cancer. 1999 Jan;7(1):39-43.
414 6. Kimura M, Araoka H, Yamamoto H, Nakamura S, Nagi M, Yamagoe S, et al. Micafungin
415 Breakthrough Fungemia in Patients with Hematological Disorders. 2018 Apr
416 26;62(5):e02183-17.
417 7. Iturrieta-González IA, Padovan ACB, Bizerra FC, Hahn RC, Colombo AL. Multiple species
418 of Trichosporon produce biofilms highly resistant to triazoles and amphotericin B. PLoS
419 One. 2014 Oct 31;9(10):e109553.
420 8. Cai YY, Li L, Zhu XM, Lu JP, Liu XH, Lin FC. The crucial role of the regulatory
421 mechanism of the Atg1/ULK1 complex in fungi. Frontiers in Microbiology. 2022 Oct
422 26;13:1019543.
423 9. Ohsumi Y. Molecular mechanism of autophagy in yeast, Saccharomyces cerevisiae. Philos
424 Trans R Soc Lond B Biol Sci. 1999 Sep 29;354(1389):1577-80; discussion 1580-1.
425 10. Wong PM, Puente C, Ganley IG, Jiang X. The ULK1 complex sensing nutrient signals for
426 autophagy activation. Autophagy. 2013 Feb 1;9(2):124-37.

427 11. Kamada Y, Funakoshi T, Shintani T, Nagano K, Ohsumi M, Ohsumi Y. JCB Report Tor-
428 mediated Induction of Autophagy Via an Apg1 Protein Kinase Complex. J Cell Biol. 2000
429 Sep 18;150(6):1507-13.
430 12. Metur SP, Klionsky DJ. Nutrient-dependent signaling pathways that control autophagy in
431 yeast. FEBS Letters. 2024 Jan;598(1):32-47.
432 13. Kitamoto K, Yoshizawa K, Ohsumi Y, Anraku2 Y. Dynamic Aspects of Vacuolar and
433 Cytosolic Amino Acid Pools of Saccharomyces cerevisiae. J Bacteriol. 1988
434 Jun;170(6):2683-6.
435 14. Suzuki K, Kubota Y, Sekito T, Ohsumi Y. Hierarchy of Atg proteins in pre-autophagosomal
436 structure organization. Genes to Cells. 2007 Feb;12(2):209-18.
437 15. Zhao X, Feng W, Zhu X, Li C, Ma X, Li X, et al. Conserved Autophagy Pathway
438 Contributes to Stress Tolerance and Virulence and Differentially Controls Autophagic Flux
439 Upon Nutrient Starvation in Cryptococcus neoformans. Front Microbiol. 2019 Nov
440 26;10:2690.
441 16. Ding H, Caza M, Dong Y, Arif AA, Horianopoulos LC, Hu G, et al. ATG genes influence
442 the virulence of Cryptococcus neoformans through contributions beyond core autophagy
443 functions. Infect Immun. 2018 Aug 22;86(9):e00069-18.
444 17. Siqi L, Liuliu J, Haochen M, Ying L, Qinqin Z, Ming M, et al. Autophagy regulation of
445 ATG13 and ATG27 on biofilm formation and antifungal resistance in Candida albicans.
446 Biofouling. 2022 Oct;38(9):926-939.
447 18. Huang Y, Yu S, Liu S, Zhao X, Chen X, Wei X. Autophagy Activated by Atg1 Interacts
448 With Atg9 Promotes Biofilm Formation and Resistance of Candida albicans. J Basic
449 Microbiol. 2025 May;65(5):e2400603.
450 19. Matsumoto Y, Yoshikawa A, Nagamachi T, Sugiyama Y, Yamada T, Sugita T. A critical
451 role of calcineurin in stress responses, hyphal formation, and virulence of the pathogenic
452 fungus Trichosporon asahii. Sci Rep. 2022 Sep 27;12(1):16126.
453 20. Matsumoto Y, Sugiyama Y, Nagamachi T, Yoshikawa A, Sugita T. Hog1-mediated stress
454 tolerance in the pathogenic fungus Trichosporon asahii. Sci Rep. 2023 Aug 19;13(1):13539.
455 21. Matsumoto Y, Nagamachi T, Yoshikawa A, Yamazaki H, Yamasaki Y, Yamada T, et al.
456 Development of an efficient gene-targeting system for elucidating infection mechanisms of
457 the fungal pathogen Trichosporon asahii. Sci Rep. 2021 Sep 14;11(1):18270.

458 22. Matsumoto Y, Nagamachi T, Yoshikawa A, Yamada T, Sugita T. A joint PCR-based gene-
459 targeting method using electroporation in the pathogenic fungus Trichosporon asahii. AMB
460 Express. 2022 Jul 14;12(1):91.
461 23. Kurakado S, Miyashita T, Chiba R, Sato C, Matsumoto Y, Sugita T. Role of arthroconidia
462 in biofilm formation by Trichosporon asahii. Mycoses. 2021 Jan;64(1):42-47.
463 24. Matsumoto Y, Kurakado S, Yamada T, Sugita T. Strategy to Identify Virulence-Related
464 Genes of the Pathogenic Fungus Trichosporon asahii Using an Efficient Gene-Targeting
465 System. Microbiology and Immunology. 2025 Feb;69(2):77-84.
466 25. Su C, Yu J, Lu Y. Hyphal development in Candida albicans from different cell states.
467 Current Genetics. 2018 Dec;64(6):1239-1243.
468 26. Cheong H, Nair U, Geng J, Klionsky DJ. The Atg1 Kinase Complex Is Involved in the
469 Regulation of Protein Recruitment to Initiate Sequestering Vesicle Formation for
470 Nonspecific Autophagy in Saccharomyces cerevisiae. Mol Biol Cell. 2008 Feb;19(2):668-
471 81.
472 27. Kirisako T, Baba M, Ishihara N, Miyazawa K, Ohsumi M, Yoshimori T, et al. Formation
473 Process of Autophagosome Is Traced with Apg8/Aut7p in Yeast. J Cell Biol. 1999 Oct
474 18;147(2):435-46.
475
476

Supporting information

S1 Dataset. Datasets included in this study.

480 **Table 1 *T. asahii* strains used in this study**

T. asahii strains	Relevant genotype	Background	Reference
MPU129 Δ*ku70* (Parent strain)	*ku70*::*nptII*	MPU129	Matsumoto Y., *et. al*. [21]
Δ*atg1* #1-#3	*ku70*::*nptII*, *atg1*::*NAT1*	MPU129 Δ*ku70*	This study

481

482 **Table 2 NCBI gene accession numbers for the Atg1 protein used to create the phylogenetic**
483 **tree**
484

Species	Definition	NCBI accession	Size (aa)	Query Cover (%)	Percent Identical (%)
Trichosporon asahii	hypothetical protein A1Q1_02656 (*Trichosporon asahii var. asahii* CBS 2479)	XP_014179392.1	995	100	100
Cryptococcus neoformans	ULK/ULK protein kinase (*Cryptococcus neoformans var. grubii* H99)	XP_012048654.1	985	98	51.87
Aspergillus fumigatus	serine/threonine protein kinase (Pdd7p), putative (*Aspergillus fumigatus* Af293).	XP_751920.1	973	77	52.33
Candida albicans	serine/threonine protein kinase (*Candida albicans* SC5314)	XP_717245.2	834	31	50.46
Saccharomyces cerevisiae	serine/threonine protein kinase ATG1 (*Saccharomyces cerevisiae* S288C)	NP_011335.1	897	61	47.45

485
486

487 **Table 3 NCBI domain accession number for the Atg1 protein.**
488

Domain name	NCBI accession	Description	Species	Interval
PKc_like super family	cl21453	Protein Kinases, catalytic domain	*Trichosporon asahii*	34-339
STKc_ATG1_ULK_like	cd14009	Catalytic domain of the Serine/Threonine kinases, Autophagy-related protein 1 and Unc-51-like kinases	*Cryptococcus neoformans* *Aspergillus fumigatus* *Candida albicans* *Saccharomyces cerevisiae*	33-336 29-327 64-350 30-324
DUF3543	pfam12063	Domain of unknown function (DUF3543)	*Trichosporon asahii* *Cryptococcus neoformans* *Aspergillus fumigatus* *Candida albicans* *Saccharomyces cerevisiae*	737-974 741-979 651-941 621-829 586-893
Herpes_BLLF1 super family	cl37540	Herpes virus major outer envelope glycoprotein	*Trichosporon asahii*	370-536

489
490

491 **Table 4 Primers used to generate *atg1* gene-deficient mutants.**
492

Primers	Nucleic acid sequence
pUC19-*NAT1* for cloning	
F *NAT1* (for 5UTR typing)	GAGCTGATACCGCTCGCCGCTGCGAGGATGTGAGCTGGAGAGC
R *NAT1* (for 3UTR typing)	GTTTCGGTGATGACGGTGGAAGAGATGTAGAAACTAGCTTCCTGGTTTCAGAG
F pUC19 (*NAT1* inf)	CACCGTCATCACCGAAACGCGC
R pUC19 (*NAT1* inf)	GGCGAGCGGTATCAGCTCACTCAAAGGCGGTAATACG
pUC19-*atg1* (5'UTR) -*NAT1*-*atg1* (3'UTR) for cloning	
pUC19-*atg1* (5'UTR) -*NAT1* (1st cloning)	
F *NAT1* (for 5'UTR typing)	GCTGCGAGGATGTGAGCTGGAGAGCGGCGC
R pUC19 (for 5'UTR typing)	GGCGAGCGGTATCAGCTCACTCAAAGGCGGTAATACG
F *atg1* (5'UTR)	GAGCTGATACCGCTCGCCGCCCATGTCTCGTCCGGTCCCAAACCTC
R *atg1* (5'UTR)	AGCTCACATCCTCGCAGCGCGTGTGGTGGGTGAGTGGGAGTGGATG
pUC19-*atg1* (5'UTR) -*NAT1*-*atg1* (3'UTR) (2nd cloning)	
F pUC19 (for 3'UTR typing)	CACCGTCATCACCGAAACGCGC
R *NAT1* (for 3'UTR typing)	GAAGAGATGTAGAAACTAGCTTCCTGGTTTCAGAGAC
F *atg1* (3'UTR)	TAGTTTCTACATCTCTTCCCCTCTGCTTCTCCTTCTTCGCCTGCGC
R *atg1* (3'UTR)	GTTTCGGTGATGACGGTGGCAAAGTCGCCTGCAAGTCGCCTGACCG
Primers-1 for *atg1* Genotyping	
F atg1 gene ORF	GGCAGAAGTTGACGAGCAAGCTGC
R atg1 gene ORF	CCGAAGCGAAGAATGCGTCGAAACC
Primers-2 for *atg1* genotyping	
F atg1 locus	GCCCATGTCTCGTCCGGTCCCAAACCTC
R atg1 locus	GCAAAGTCGCCTGCAAGTCGCCTGACCG
Primers-3 for *atg1* genotyping	
F atg1 gene outside	CGACCGACACAGAATTGAGCCACAAC
R atg1 gene outside	CTGGTGCGGTACCGGTAAGCCGTGTCGTCAAG

493
494

495 **Table 5 MIC values of *atg1* gene-deficient mutants against antifungal agents.**
496

MIC (μg/mL)	Parent	*Δatg1* #1	*Δatg1* #2	*Δatg1* #3
MCFG	>16	>16	>16	>16
CPFG	4	4	4	4
AMPH-B	0.5	0.5	0.5	0.5
5-FC	>64	>64	>64	>64
FLCZ	1	1	1	1
ITCZ	0.5	0.5	0.5	0.5
VRCZ	0.12	0.12	0.12	0.12
MCZ	0.5	0.5	0.5	0.5

497

498 The *T. asahii* parental strain (Parent) and three independent *atg1* gene-deficient mutant *T. asahii*
499 strains (Δ*atg1* #1-3) were cultured in Sabouraud medium for 2 days at 27 °C. *T. asahii* cells were
500 suspended in saline, and cell suspensions were prepared to a turbidity of 1 according to the
501 McFarland turbidity method. Each bacterial solution was diluted 20-fold in saline and then 100-
502 fold in RPMI MOPS. The prepared fungal solutions were then diluted with eight antifungal agents
503 (Micafungin [MCFG], caspofungin [CPFG], amphotericin B [AMPH-B], 5-fluorocytosine [5-FC],
504 fluconazole [FLCZ], itraconazole [ITCZ], voriconazole [VRCZ], miconazole [MCZ]) and
505 inoculated on plates at 37°C for 48 h. The minimum inhibitory concentration (MIC) was
506 determined from the results of two independent experiments.
507

Figure 1

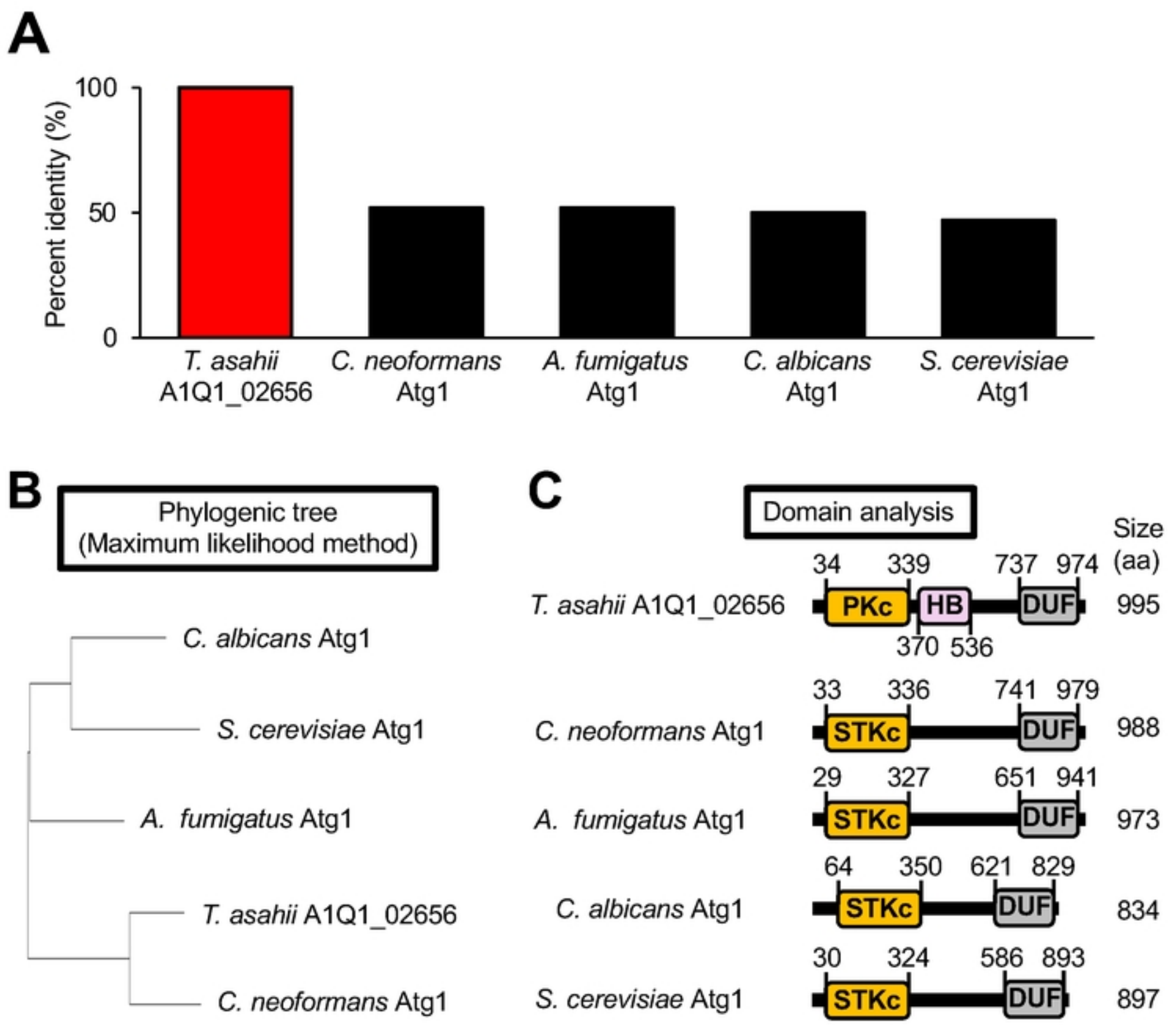

Fig. 1. Conservation of *T. asahii* Atg1 among fungi.
(**A**) Phylogenetic tree of Atg1 proteins from *T. asahii*, *C. neoformans*, *A. fumigatus*, *C. albicans*, and *S. cerevisiae*, constructed using the maximum likelihood method. (**B**) Phylogenetic tree of Atg1 proteins from *T. asahii*, *C. neoformans*, *A. fumigatus*, *C. albicans*, and *S. cerevisiae*, constructed using the maximum likelihood method. Phylogenetic analysis was performed using MEGA11 Software (https://www.ncbi.nlm.nih.gov/). (**C**) Schematic diagrams of domains present in Atg1 proteins. PKc: PKc_like superfamily domain. STKc: STKc_ATG1_ULK_like domain. HB: Herpes_BLLF1 superfamily domain. DUF: DUF3543. Functional domain prediction was performed using the National Center for Biotechnology Information (NCBI) (https://www.ncbi.nlm.nih.gov/).

Figure 2

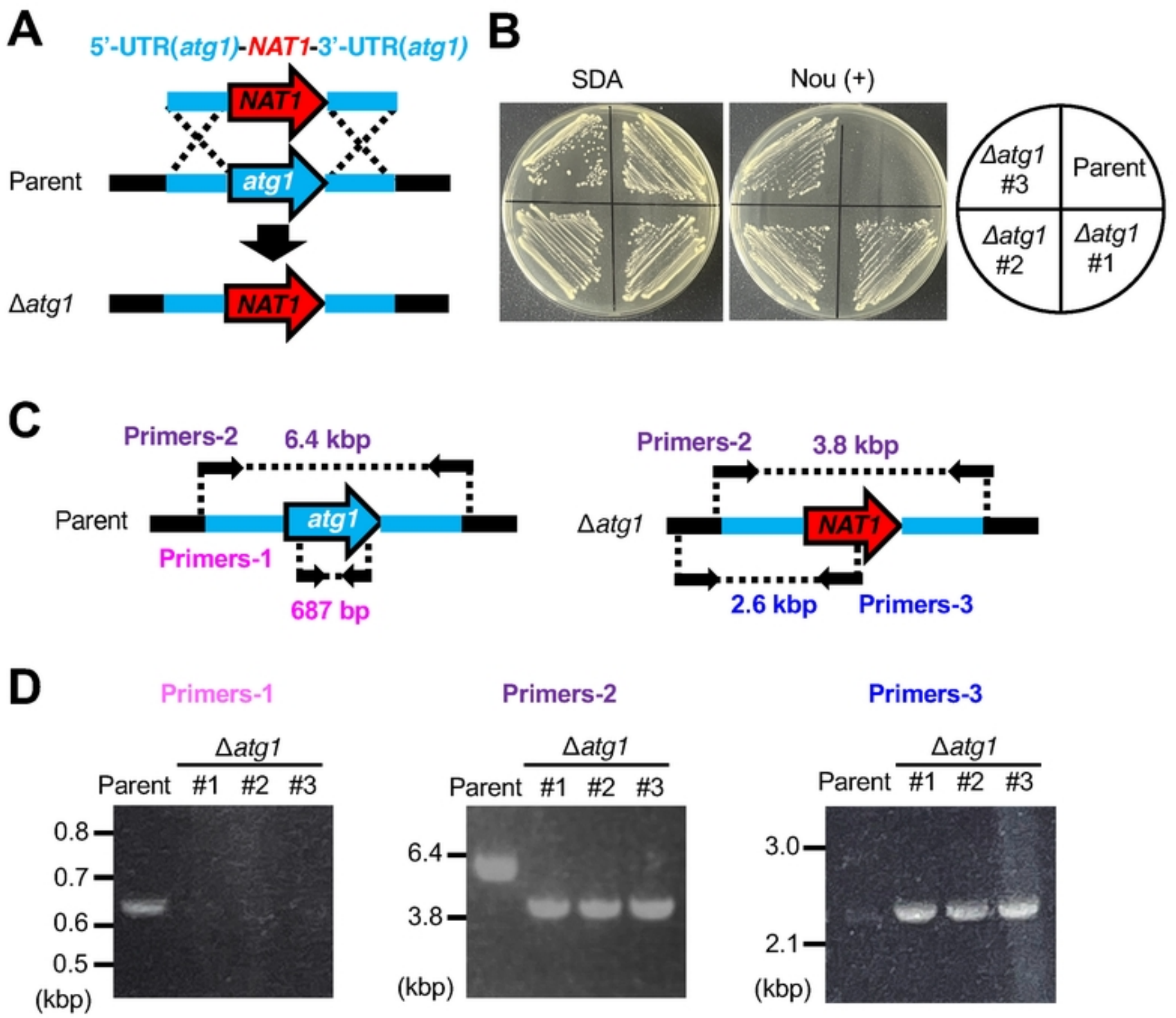

Fig. 2. Generation of the *atg1* gene-deficient *T. asahii* mutants.
(**A**) Schematic diagram of the gene recombination strategy used to construct the *atg1* gene-deficient *T. asahii* mutant (Δ*atg1*), along with the predicted genomic structure of the *atg1* gene-deficient mutant. (**B**) The parental strain (Parent) and the *atg1* gene-deficient mutants (Δ*atg1* #1-3) were spread on SDA or SDA containing nourseothricin (100 μg/mL; Nou (+)) and incubated at 27° C for 2 days. (**C**) Schematic illustration of primer positions and expected amplified DNA fragment sizes by PCR to verify the genomic structure of the *atg1* gene-deficient candidates using extracted genomic DNA. (**D**) DNA electrophoresis of PCR products to confirm the *atg1* gene deficiency (Δ*atg1*).

Figure 2

Figure 3

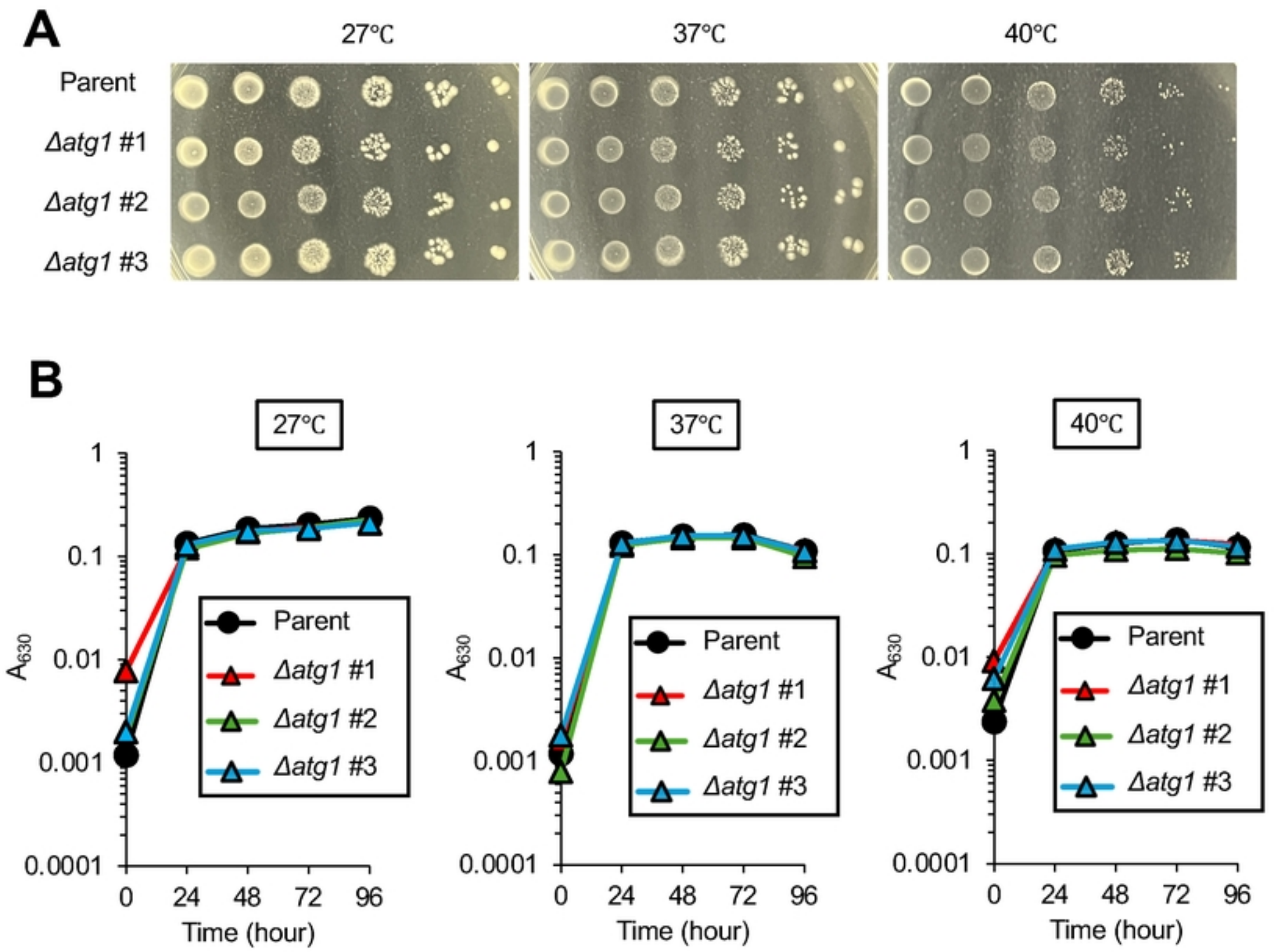

Fig. 3. Growth of the *atg1* gene-deficient *T. asahii* mutants under high-temperature conditions. (**A**) The parental strain (Parent) and the *atg1* gene-deficient *T. asahii* mutants (Δ*atg1* #1-3) were grown on SDA at 27° C for 2 days. Cells were suspended in saline, and 10-fold serial dilutions were prepared. Each dilution (5 μl) was spotted onto SDA and incubated at 27° C, 37° C, or 40° C for 48 h. (**B**) The parental strain (Parent) and the *atg1* gene-deficient *T. asahii* mutants (Δ*atg1* #1-3) were grown in Sabouraud dextrose broth at 27° C, 37° C, or 40° C, and absorbance at 630 nm was measured. Data are presented as mean ± standard error of the mean (SEM).

Figure 3

Figure 4

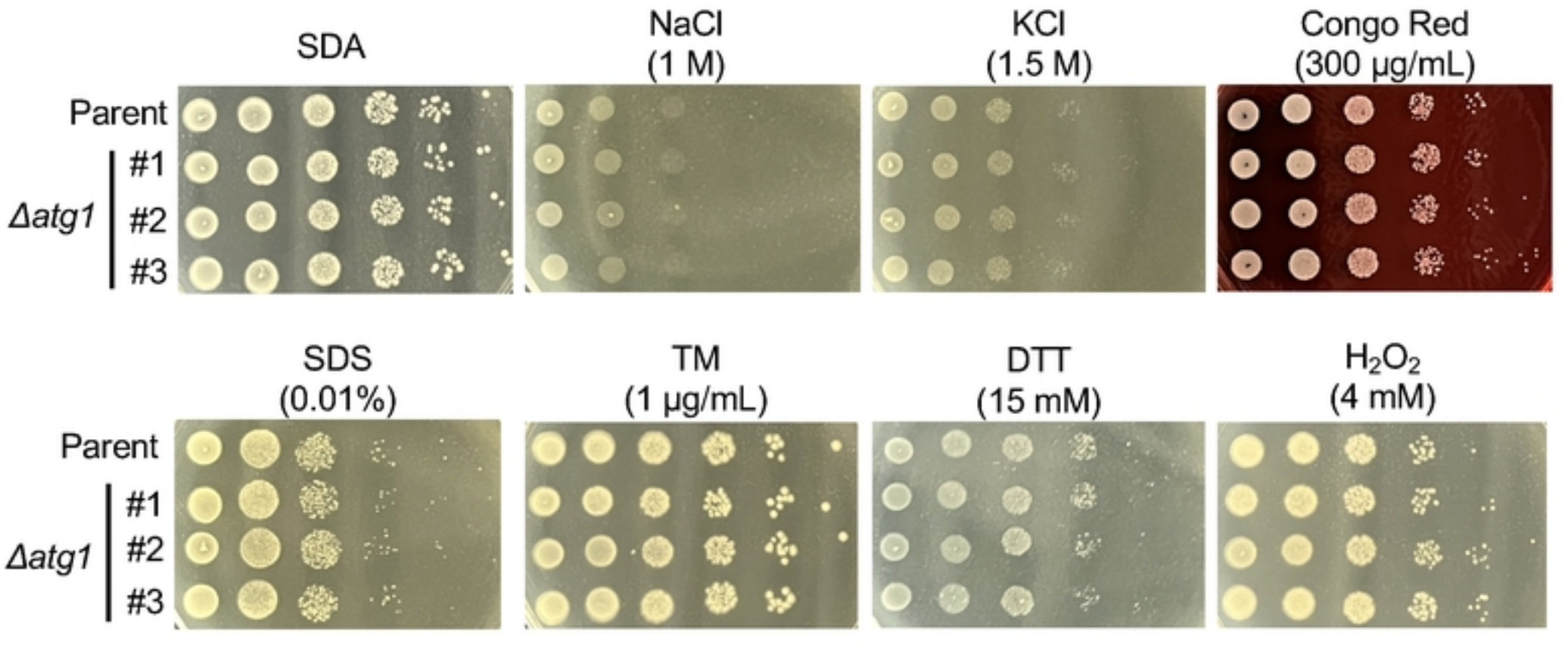

Fig. 4. Growth of the *atg1* gene-deficient *T. asahii* mutants under stress-inducing conditions. The parental strain (Parent) and the *atg1* gene-deficient *T. asahii* mutants (Δ*atg1* #1-3) were cultured on SB at 27° C for 2 days. Cells were suspended in saline, and 10-fold serial dilutions were prepared. Each dilution (5 μL) was spotted onto SA medium containing NaCl (1 M), KCl (1.5 M), Congo red (300 μg/mL), SDS (0.01%), tunicamycin (TM, 1 μg/mL), dithiothreitol (DTT, 15 mM), or hydrogen peroxide (H_2O_2, 4 mM), and incubated at 27° C for 48 h.

Figure 4

Figure 5

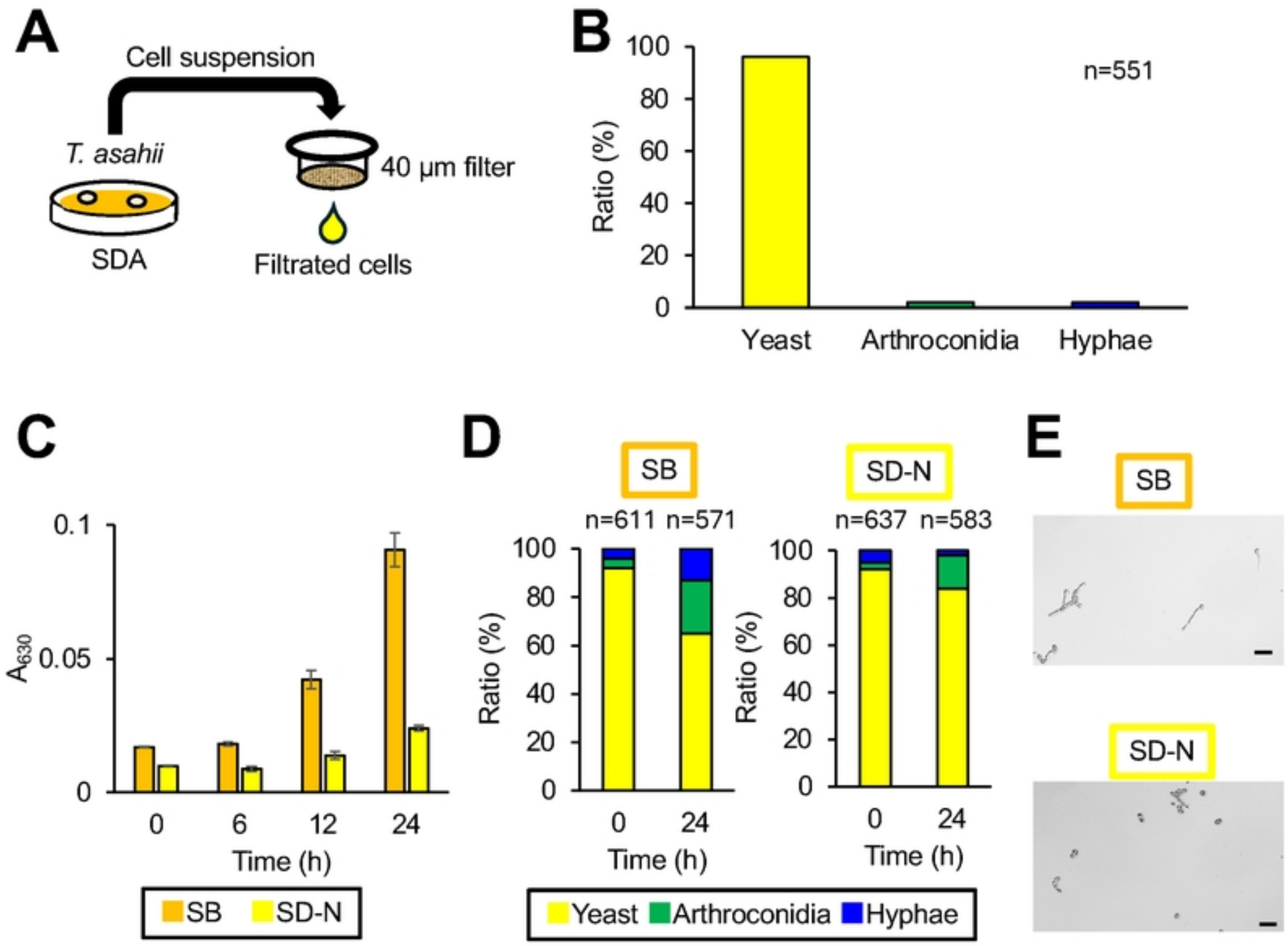

Fig. 5 Effects of culture conditions on *T. asahii* morphology.
(**A**) Method for preparing the yeast form of *T. asahii*. The parental *T. asahii* strain (Parent) was cultured on SDA at 27° C for 2 days. *T. asahii* cells were suspended in saline and filtered through a 40-μm cell strainer. (**B**) The ratio of each cell shape in the filtered *T. asahii* cells was measured. (**C**) Absorbance of the cell suspension at 630 nm was adjusted to 0.5, and 5 μL of the filtered cell suspension was added to 200 μL of Sabouraud dextrose medium or SD-N liquid medium. Cultures were incubated at 27° C for 24 h, and absorbance at 630 nm was measured for 24 h. (**D-F**) Absorbance of the filtered cell suspension at 630 nm was adjusted to 1.0, and 20 μL of the suspension was added to 200 μL of Sabouraud dextrose broth (SB) or synthetic defined-nitrogen (SD–N) medium, followed by incubation at 27° C for 24 h. Cells were then observed under a light microscope. Scale bars represent 40 μm. Images were captured randomly from multiple microscopic fields. Cell numbers in three morphologic categories,: yeast, arthroconidia, and hyphae, were quantified. (**D**) Cell numbers in three morphologic categories were measured at 0 or 24 h after incubation at 37° C. (**E**) Photographs of cells after incubation at 37° C for 24 h were obtained under microscopic fields. *n* represents the total number of microscopic fields analyzed from two independent experiments.

Figure 5

Figure 6

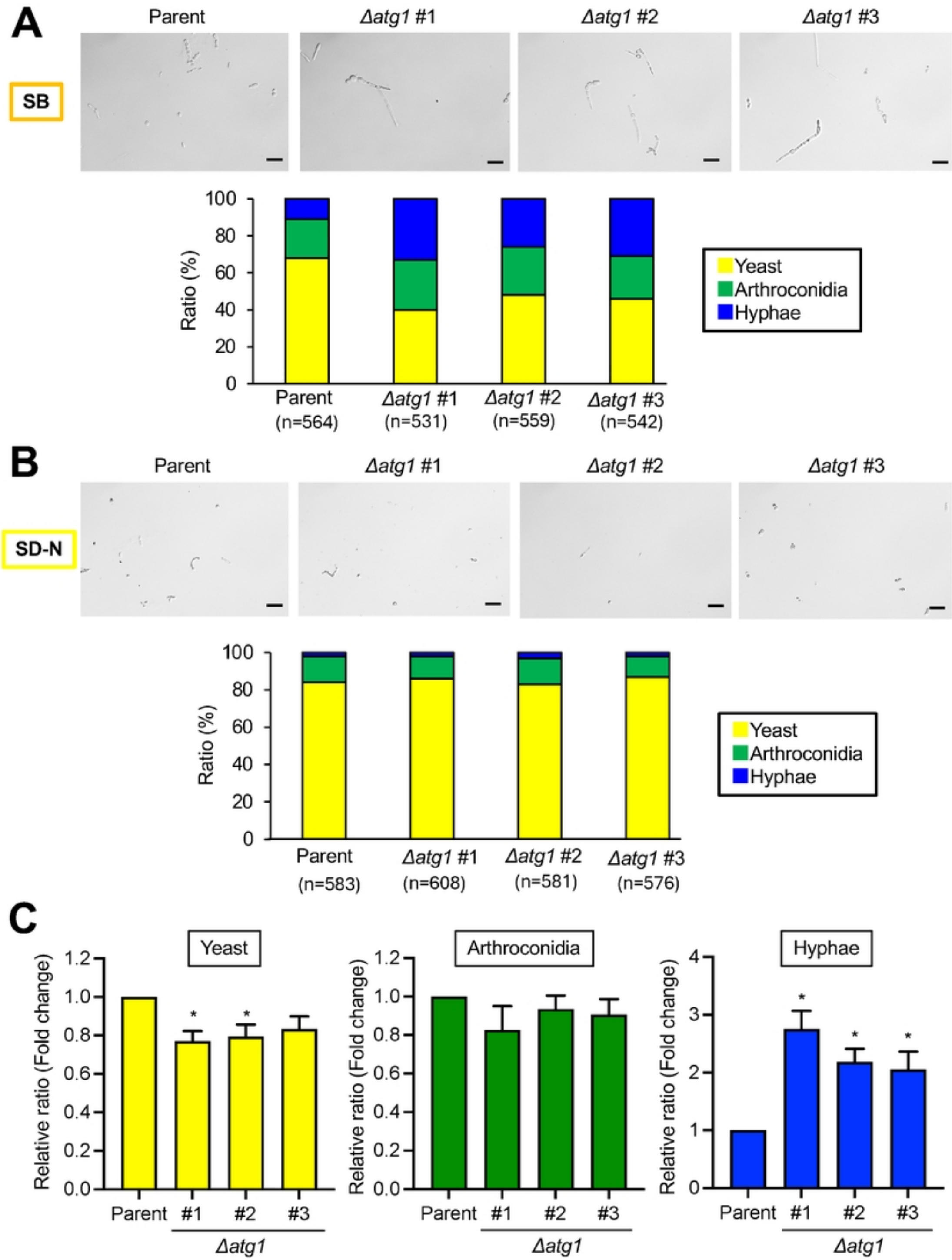
A
Parent
Δatg1 #1
Δatg1 #2
Δatg1 #3
SB
Ratio (%)
100
80
60
40
20
0
Parent (n=564)
Δatg1 #1 (n=531)
Δatg1 #2 (n=559)
Δatg1 #3 (n=542)
Yeast
Arthroconidia
Hyphae
B
Parent
Δatg1 #1
Δatg1 #2
Δatg1 #3
SD-N
Ratio (%)
100
80
60
40
20
0
Parent (n=583)
Δatg1 #1 (n=608)
Δatg1 #2 (n=581)
Δatg1 #3 (n=576)
Yeast
Arthroconidia
Hyphae
C
Yeast
Arthroconidia
Hyphae
Relative ratio (Fold change)
1.2
1.0
0.8
0.6
0.4
0.2
0.0
4
3
2
1
0
*
Parent
#1
#2
#3
Δatg1

Figure 6-continued

Fig. 6. Effect of *atg1* gene deficiency on *T. asahii* morphology.
The parental *T. asahii* strain (Parent) and three *atg1* gene-deficient mutants (Δ*atg1* #1-3) were grown on SDA at 27° C for 2 days. Cells were suspended in saline and filtered through a 40-μm cell strainer. Absorbance at 630 nm was adjusted to 1. A 20-μL aliquot of each suspension was added to (**A**) Sabouraud dextrose broth (SB), or (**B**) synthetic defined-nitrogen (SD–N) medium (200 μL). The samples were incubated at 37° C for 24 h. After incubation, the *T. asahii* cells were dropped onto microscope slides, covered with coverslips, and observed under a light microscope. Upper panels show representative microscopic images. Scale bars represent 20 μm. Lower panels show quantification of the three morphologic forms—yeast, arthroconidia, and hyphae—based on randomly selected microscopic fields. The total number of cells was obtained from two independent experiments. (**C**) The relative ratio of the three morphologic forms were determined compared to the ratio of parental strain (Parent) under a culture condition with SB at 37° C for 24 h. The data of the relative ratio were obtained from seven independent experiments. Error bars indicate the SEM of the means (n = 7). Statistical differences between parental strain and Δ*atg1* #1-3 were analyzed by Dunnett's test. (*: $P < 0.05$).

Figure 7

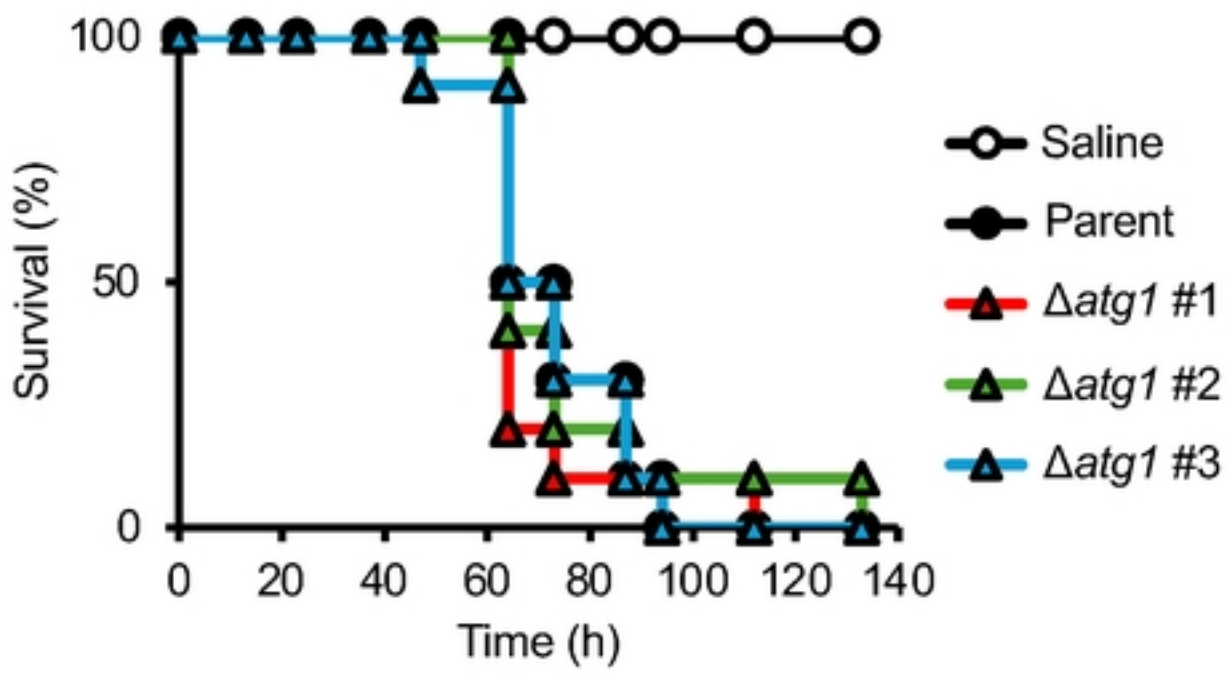

Fig. 7. Virulence of *T. asahii atg1* gene-deficient mutants in a silkworm infection model.
The parental strain (Parent; 530 cells/larva) and three independent *atg1* gene-deficient *T. asahii* mutants (Δ*atg1* #1-3; 790 - 950 cells/larva) were injected into the hemocoel of silkworms, and survival was monitored at 37° C for 96 h. Statistical significance between the parental and *atg1*-deficient groups was determined by the log-rank test based on Kaplan–Meier survival curves. Ten silkworms per group were used.

Figure 7